Faculté de physique et ingénierie
Université de Strasbourg
Institut Pluridisciplinaire Hubert Curien Strasbourg

CHARACTERIZATION AND FEASIBILITY STUDIES FOR COINCIDENT FAST-TIMING FUSION MEASUREMENTS

Mykalin Jones

Advised by Marcel Heine

For the completion of the M2-PSA

QMat Quantum Science and Nanomaterials

Outline

- Stellar Nucleosynthesis
- Reaction Rates
- 12C+12C
    - Significance
    - Challenges in cross section measurement

- Cross sections: features
- The STELLA Experiment
- PIXEL detector Characterisation
- Outlook: Simulation work

Stellar Nucleosynthesis

- Stellar evolution determined by mass
- Massive enough stars will fuse elements to iron peak
- Determines elemental abundance in the universe
- Studies relevant to:
    - Astrophysics- stellar evolution
    - Biology-source of carbon
    - Nuclear physics- molecular states

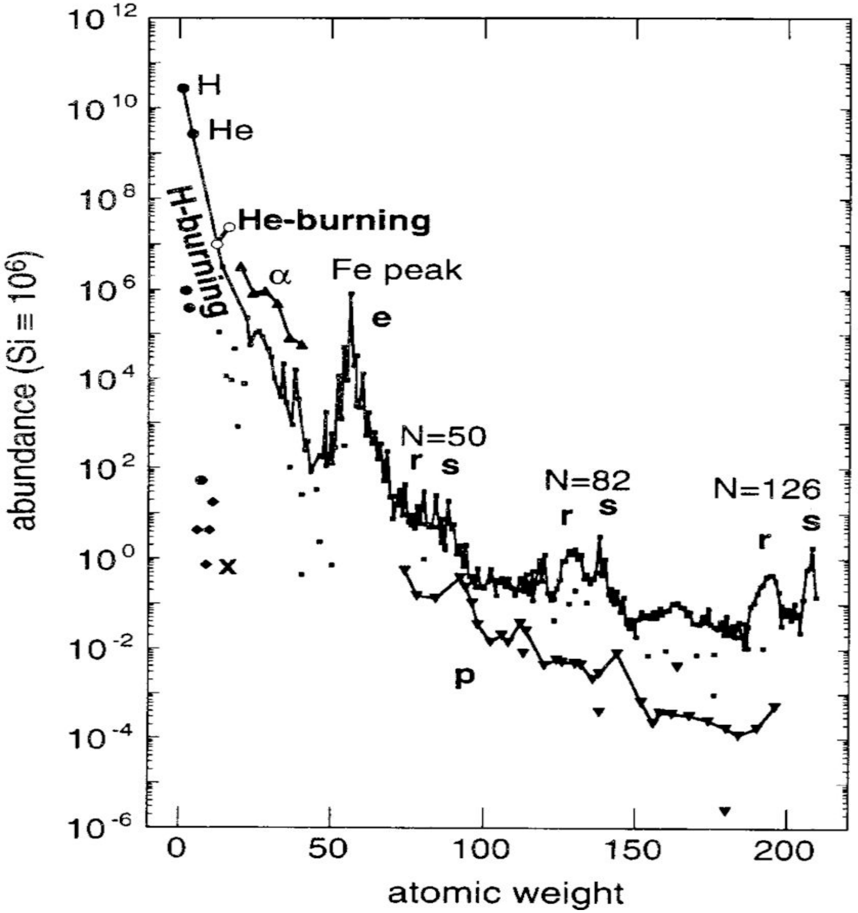

Ireland, Trevor. (1996). Isotopic anomalies in extra terrestrial grains. Journal of the Royal Society of Western Australia. 79 Pt 1. 43-50.

Reaction Rates

- Energy available from thermal motion
- T~15x10^{6}K (eg our sun) ⟶ $kT \sim 1\text{keV}$
    - During static burnings $kT \ll E_{coul}$
- Charged Particles ⟶ Coulomb barrier
- Reactions occur via Tunnel effect

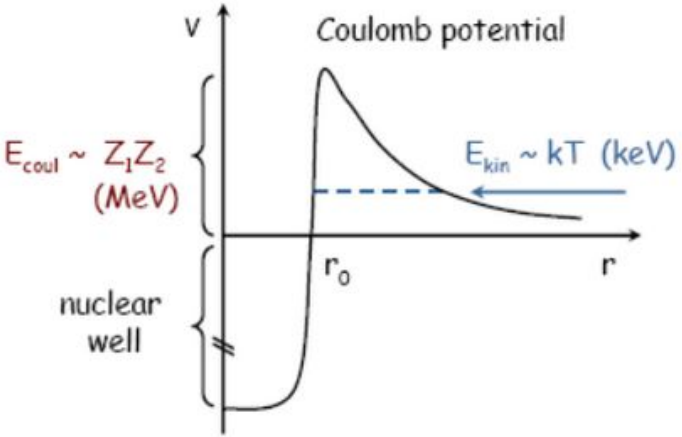

tunneling probability $\boxed{P \propto \exp(-2\pi\eta)}$

$$\boxed{\sigma(E) = \underbrace{\frac{1}{E}\exp(-2\pi\eta)}\ \underbrace{S(E)}}$$

non-nuclear origin
STRONG energy dependence

nuclear origin
WEAK energy dependence

ASTROPHYSICAL S(E)-FACTOR

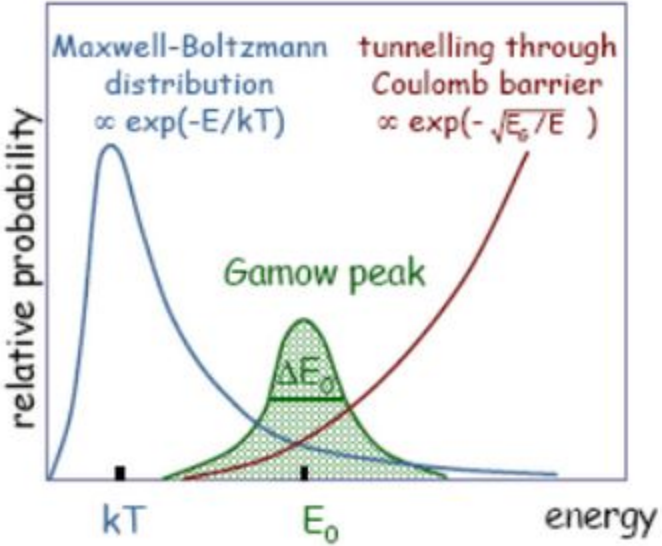

Images provided by S. Courtin

Carbon-12 + Carbon-12

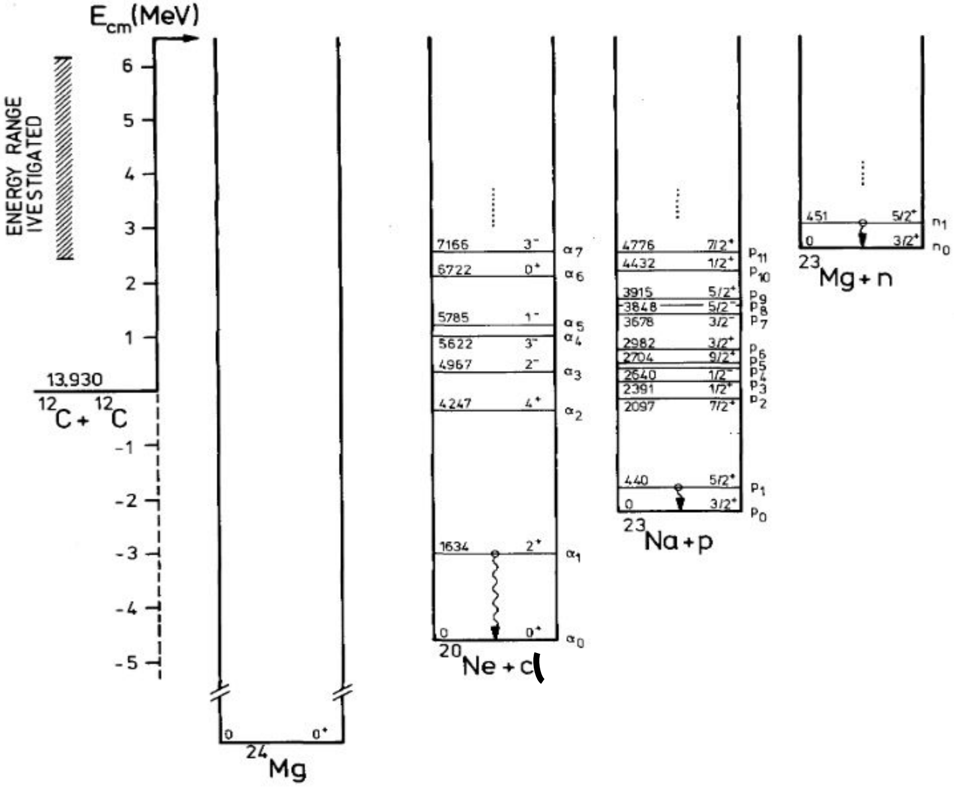

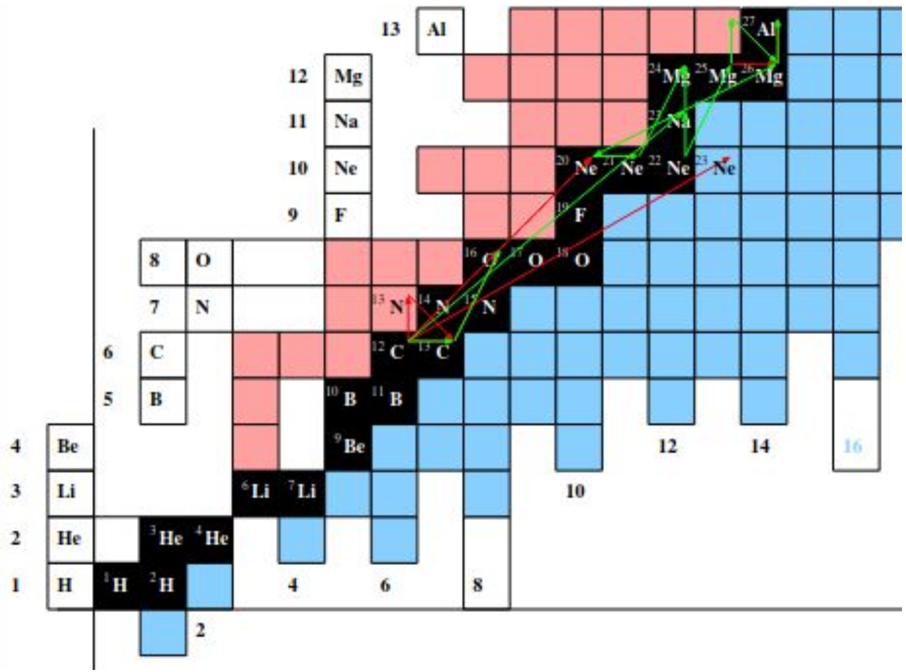

$$^{12}\mathrm{C}(^{12}\mathrm{C}, p)^{23}\mathrm{Na} \quad (Q = 2241\,\mathrm{keV})$$
$$^{12}\mathrm{C}(^{12}\mathrm{C}, \alpha)^{20}\mathrm{Ne} \quad (Q = 4617\,\mathrm{keV})$$
$$^{12}\mathrm{C}(^{12}\mathrm{C}, n)^{23}\mathrm{Mg} \quad (Q = -2599\,\mathrm{keV})$$

Kettner, K.U., ”The12C+12C Reaction at Subcoulomb Energies.” InZeitschrift fr PhysikA Hadrons and Nuclei, 65-75. Springer Berlin / Heidelberg, 1980.

Compound Nuclear Reactions and Resonances

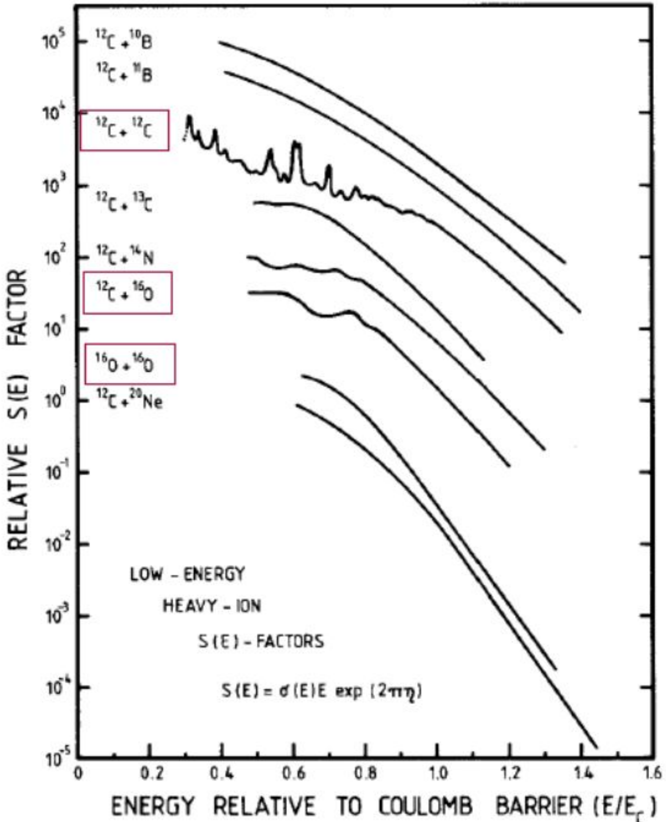

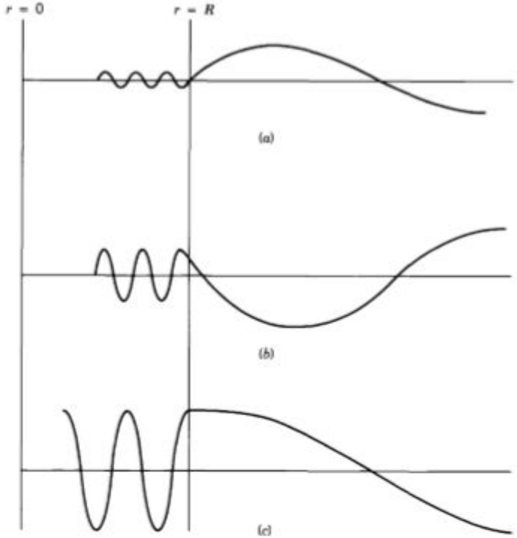

Figure 11.25 (*a*) Far from resonance, the exterior and interior wave functions match badly, and little penetration of the nucleus occurs. (*b*) As the match improves, there is a higher probability to penetrate. (*c*) At resonance the amplitudes match exactly, the incident particle penetrates easily, and the cross section rises to a maximum.

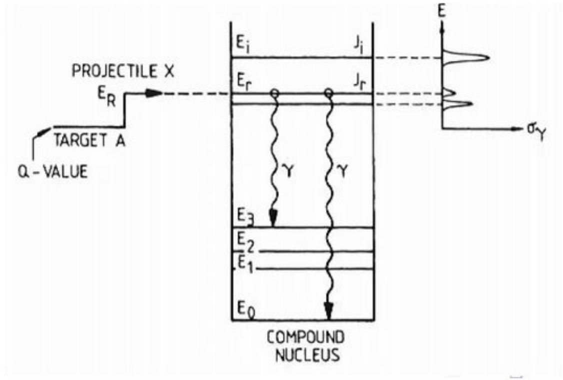

Krane, pg. 425

Fusion Hindrance

- heavy-ion fusion hindrance at extreme sub-barrier energies has been found
- first observed in medium mass systems for the fusion reaction 64Ni+ 64Ni
- excitation function σ(E) drops much faster at very low energies than predicted by standard coupled-channels (CC) calculations
- Interesting behaviour to probe

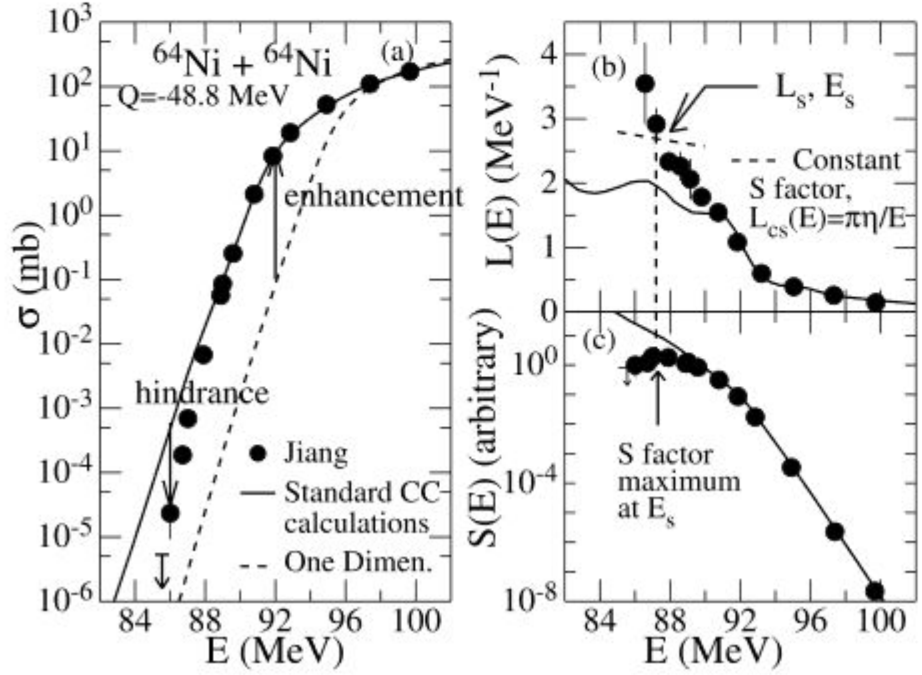

Experiments: The STELLA Apparatus

Goals:

- Make direct cross section measurements of carbon burning reaction rates
- Challenge: relevant cross sections are well below nanobarn level
- Background suppression: measure coincidences between emitted charged particles and gamma rays

Key Aspects:

- Rotating targets
- High efficiency particle and gamma detection system
- Nanosecond timing
- Employment of coincidence technique

$$^{12}\mathrm{C} + ^{12}\mathrm{C} \rightarrow ^{20}\mathrm{Ne}^{*} + \alpha$$

$$^{12}\mathrm{C} + ^{12}\mathrm{C} \rightarrow ^{23}\mathrm{Na}^{*} + \mathrm{p}$$

$$^{12}\mathrm{C} + \mathrm{d} \rightarrow ^{13}\mathrm{C}^{*} + \mathrm{p}$$

$$^{12}\mathrm{C} + \mathrm{H} \rightarrow ^{12}\mathrm{C} + \mathrm{H}$$

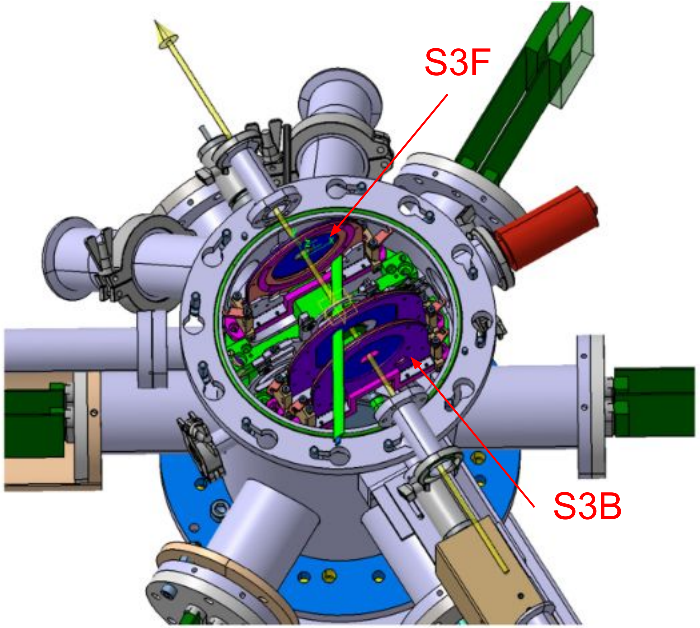

Two S3 type detectors: Front-most S3 is denoted S3F (forward) and the rear-most S3B (backward).

Resource: “The STELLA apparatus for particle-Gamma coincidence fusion measurements with nanosecond timing”, 22/2/2018, M. Heine, S. Courtin, et. al

Angular Acceptance

- Benefit to increasing angular acceptance
- Would require placement of third detector
- Limited space inside chamber

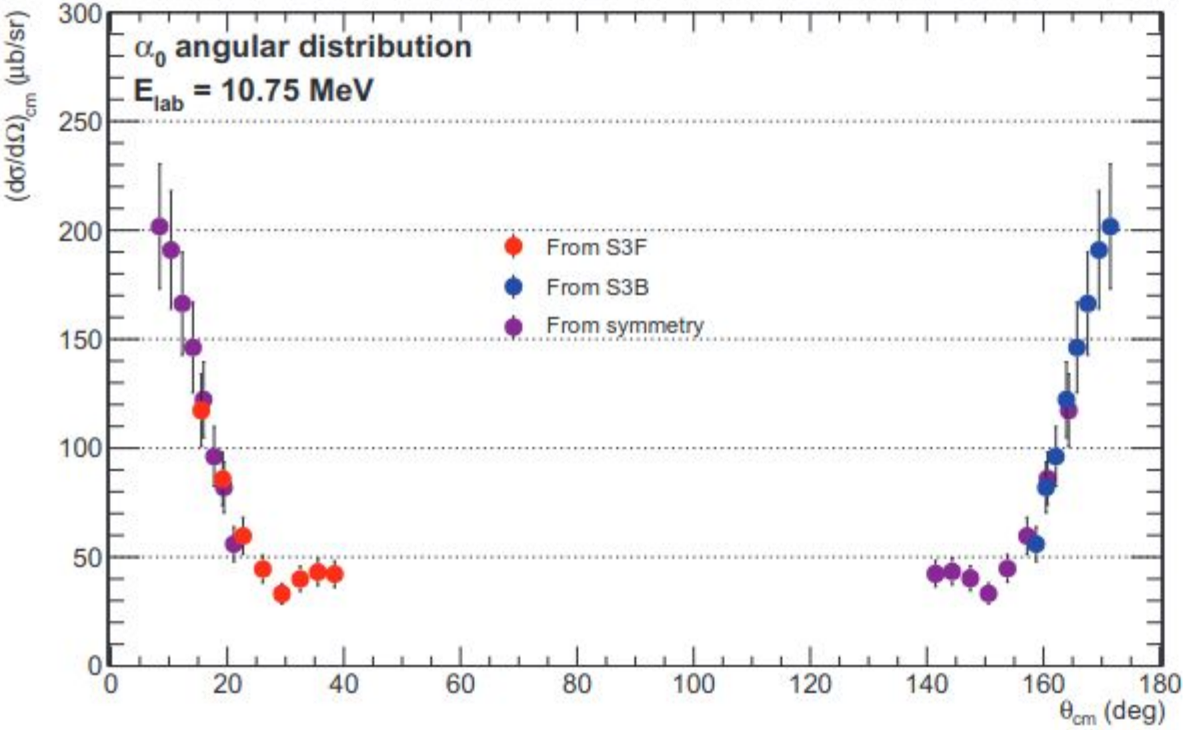

Angular distribution of α_0 at E_{lab} = 10.75 MeV obtained with the S3B detector (blue points) and S3F detector (red points), while the points in purple represent their symmetry with respect toθcm = 90◦.

Fruet,Guillaume 2018, ED182

Experimental Setup

- 1cm x 3mm pixel
- Ohmic side sectors: surface
- Junction side strips:recombine for total energy

- S^3 test bench:
- Placement of triple alpha source
  - 2.5cm +/- 1mm from detector
  - 6 point mesh for collimation
  - T= 25C, allows for time stable measurements
  - Measurement time 1-2 days

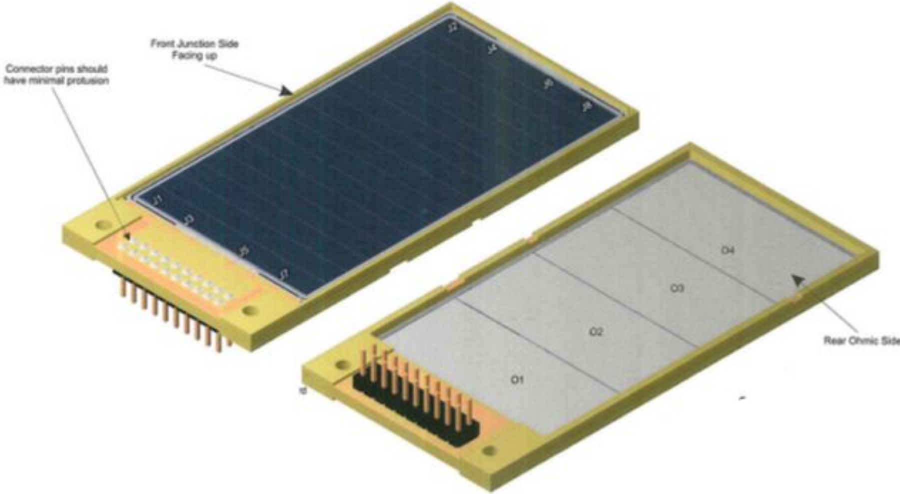

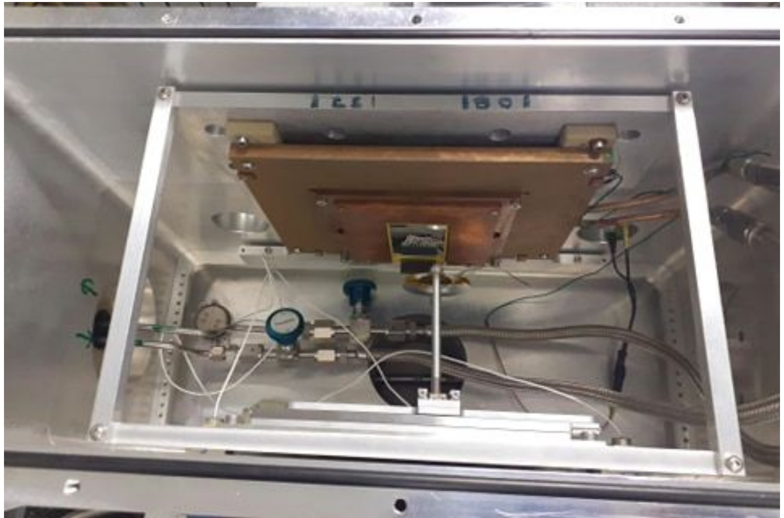

The Signal

- Junction side left
- Ohmic upper right

- J1+J2, fitting gives resolution
- Fitting ohmic → energy calibration
- Source position:

run 1, x=16.6mm, y=14mm

- lower rh side, Q2

Junction 1

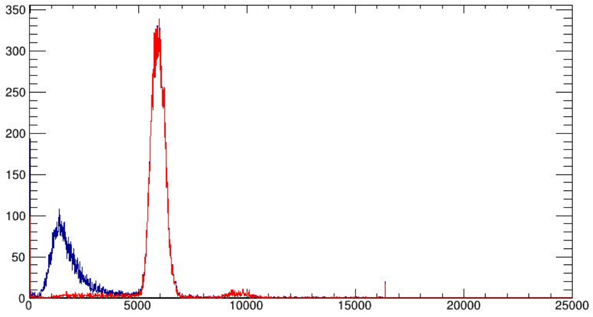

Ohmic side

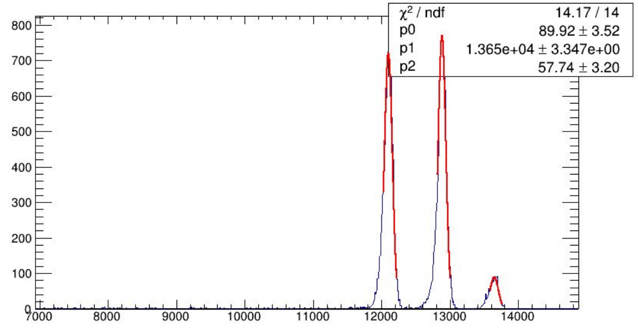

Junction 2

counts

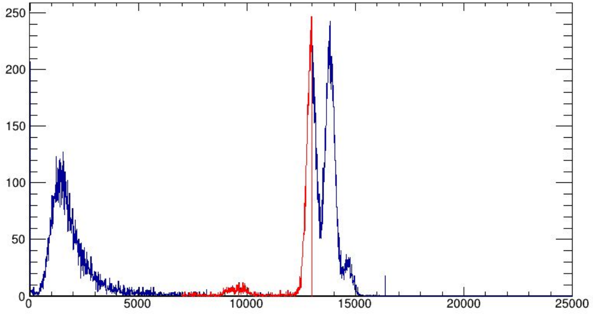

Junction 1 + Junction 2

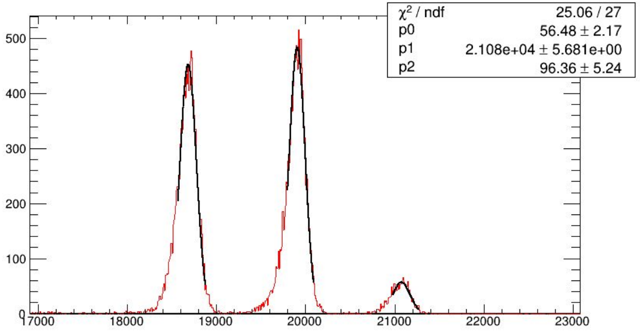

Energy channel

Energy Calibration

- Using parameters from ohmic histogram fitting and values from nudat for energies
- Establish: offset, slope
- Apply to data

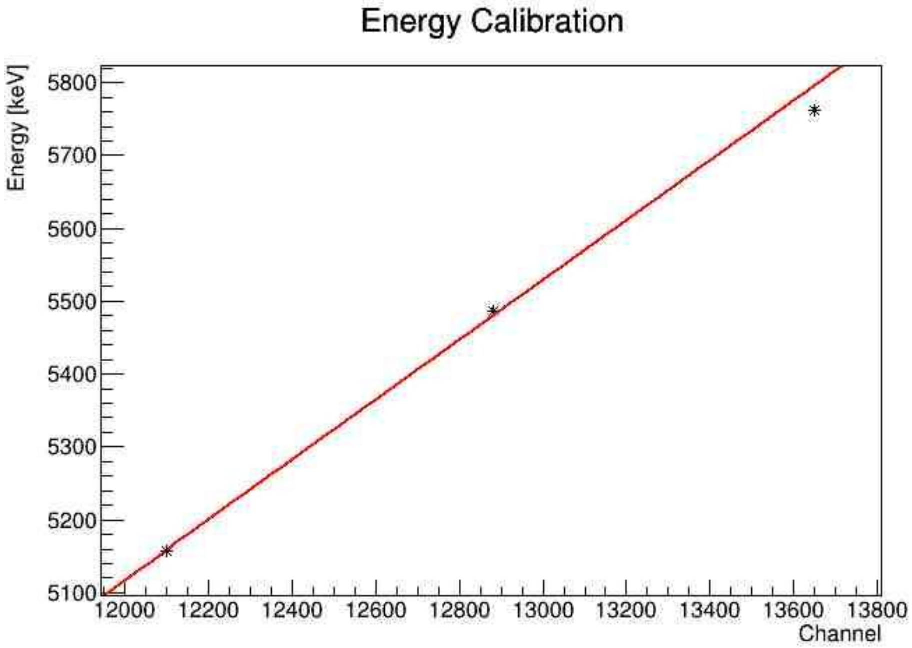

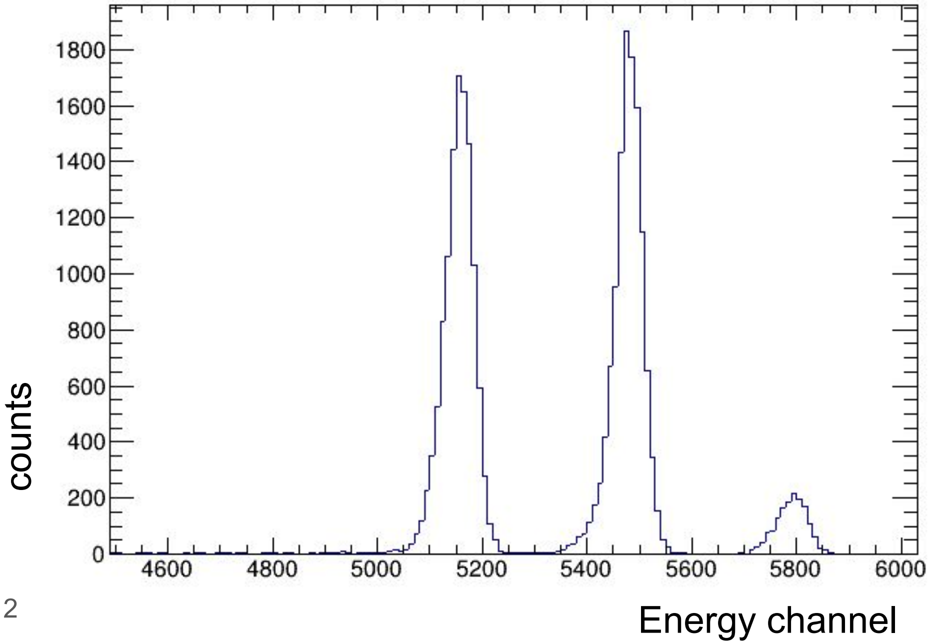

Double gauss fitting procedure

- Compared to single gauss fitting procedure
- Contribution of secondary peaks for Plutonium most significant
- Overall, single gauss fitting procedure yielded better fitting results

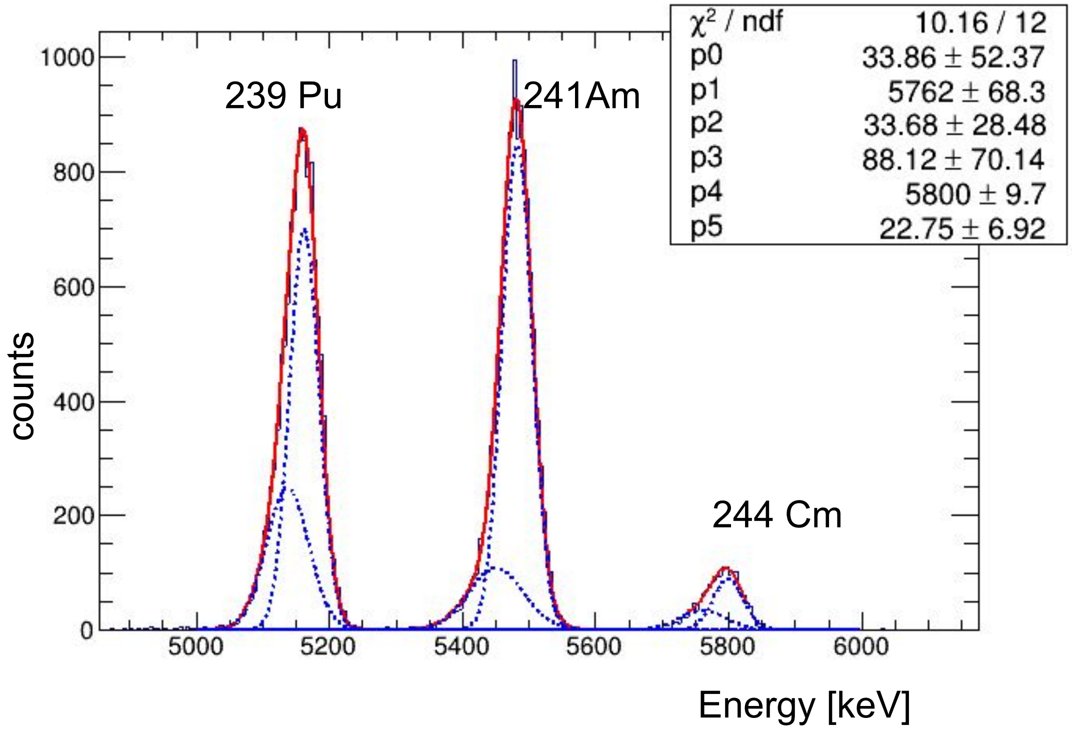

Procedure

1. Fit Ohmic side, Junction side, and combined plot for energy resolution comparison
2. Repeated procedure for 3 positions
3. Plot and fit the energy difference and the time difference at junctions for each position
4. Calculated the spatial resolution from the time domain and energy domain

Correlation between ohmic side and total junction side

"Combined plot"

Features:

- Peaks associated with triple alpha source
- Line corresponds to energy loss, same for both sides

⟶ Before entering detector

- Along junction axis peaks

⟶ May fail to hit sector

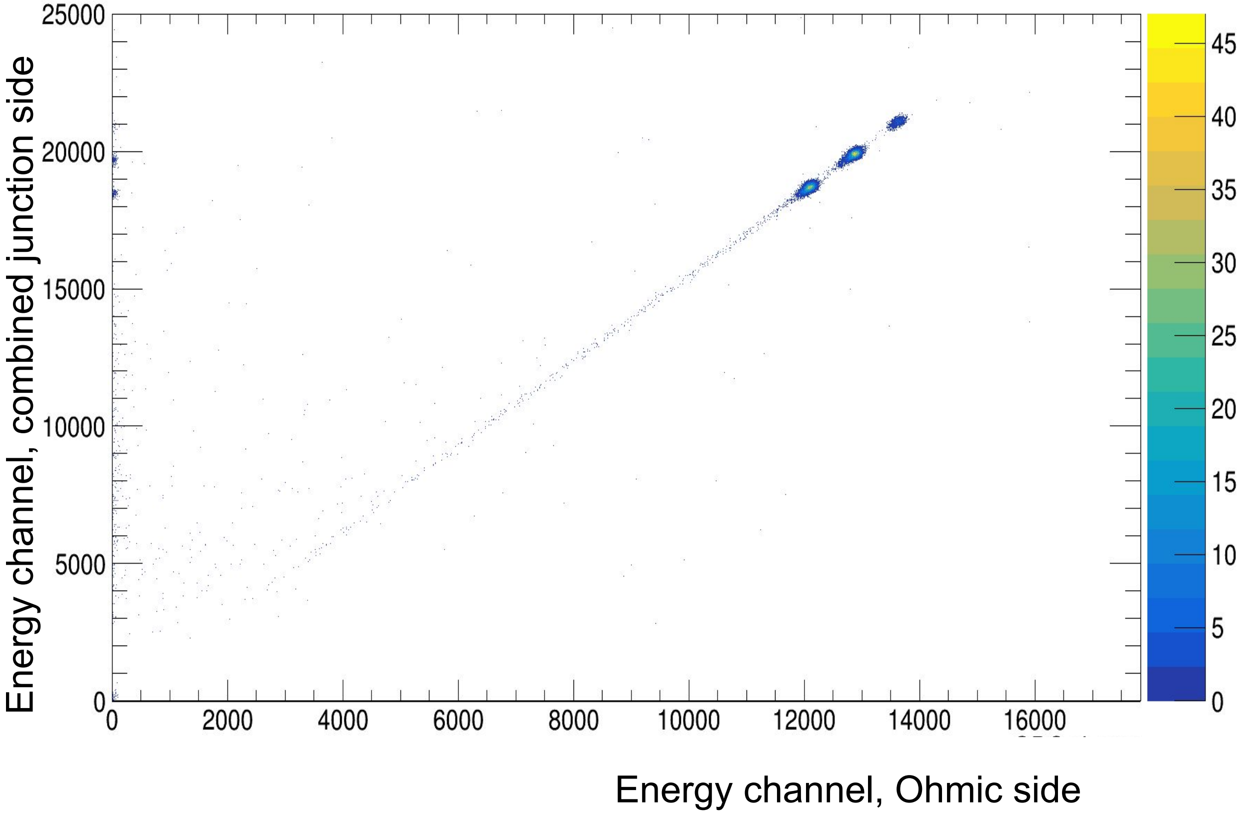

Fitting of correlation plot and projection plot

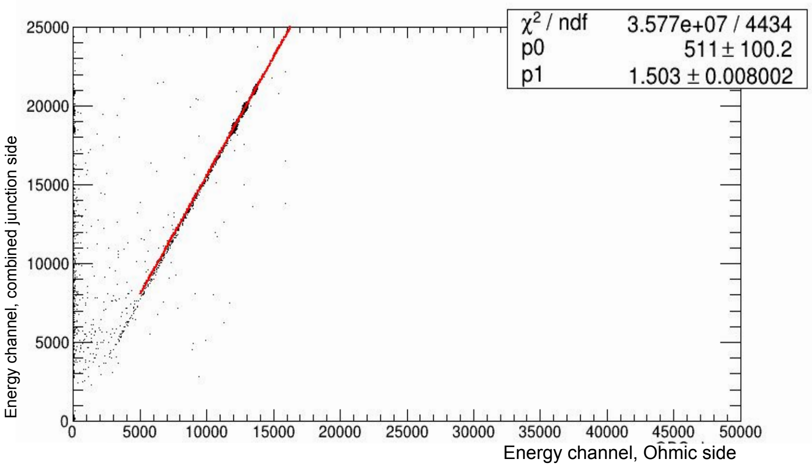

- Linear fit on correlation plot
- Projected onto x-axis
- Applied fitting routine

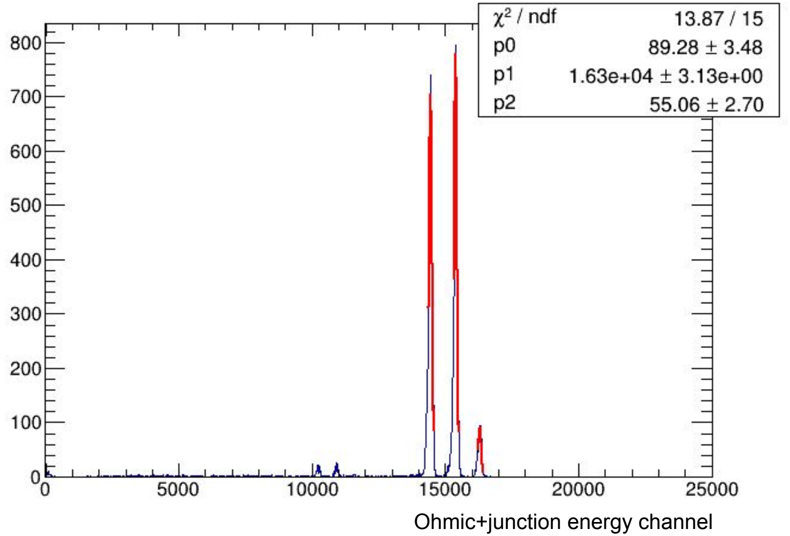

Energy Resolution by Source Position

- Americium peaks compared
- Small fluctuations in relative resolution on junction side
- Ohmic side generally better
- Increased uncertainty on run three ohmic side

Side	run/peak	Mean	Uncertainty	Sigma	Uncertainty	Relative resolution
Junction	1/2	19909.3	1.4	88.62	1.4	$(4.45 \pm 0.07) \times 10^{-1}$
Junction	2/2	19717.4	1.2	89.7	1.2	$(4.55 \pm 0.06) \times 10^{-1}$
Junction	3/2	19761.7	1.3	94.2	1.3	$(4.77 \pm 0.07) \times 10^{-1}$
Ohmic	1/2	12884.09	1.0	57.20	1.0	$(4.44 \pm 0.08) \times 10^{-1}$
Ohmic	2/2	12624.56	.50	41.00	.48	$(3.25 \pm 0.04) \times 10^{-1}$
Ohmic	3/2	12809.46	2.8	52.40	3.0	$(4.1 \pm 0.2) \times 10^{-1}$

Energy Resolution by Detector Side

- Here the Americium peak is shown
- Selected the second run with best measurements
- Ohmic side is better than junction side due to propagation of uncertainties
- Combined plot has best resolution because it contains more information

Side	run/peak	Mean	Uncertainty	Sigma	Uncertainty	Relative resolution
Junction	2/2	19717.4	1.2	89.7	1.2	$(4.55\pm0.06)\times10^{-1}$
Ohmic	2/2	12624.56	.50	41.00	.48	$(3.25\pm0.04)\times10^{-1}$
Combined	2/2	15160.33	.64	48.72	.62	$(3.21\pm0.04)\times10^{-1}$

Position Resolution

- Calculated a scaling factor from the three positions for time and energy
- Picked with lowest uncertainty
- Applied to data to calculate mean, standard deviation and uncertainties
- Not enough bins for timing fit to be reliable
- Faster DAQ would increase binning

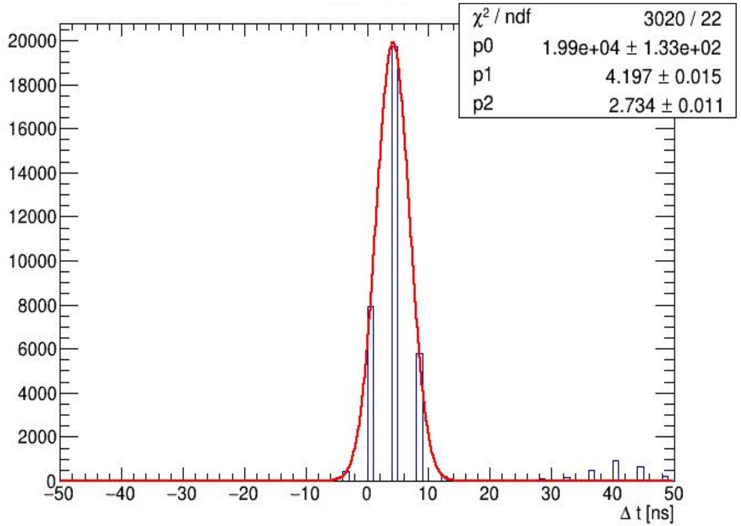

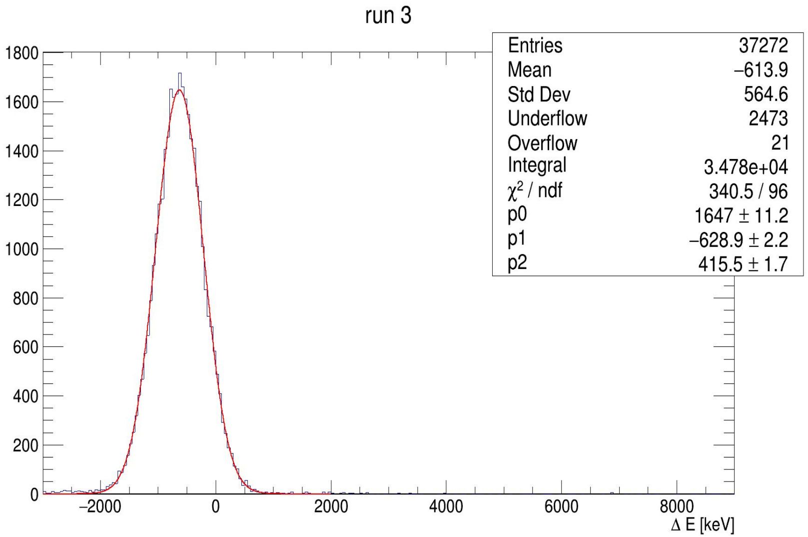

Time domain versus Energy domain

- Agreement within uncertainties on measurements in energy domain
- Better resolution with energy domain
    - Best at central position

Time

Run number	Sd (mm)	uncertainty	Relative uncertainty
1(lower)	2.18	.03	1.38%
2(upper)	1.80	.03	1.67%
3 (central)	1.66	.02	1.20%

Energy

Run number	Sd (mm)	uncertainty	Relative uncertainty
1(lower)	1.45	±0.02	1.75%
2(upper)	1.41	±0.02	1.41%
3 (central)	1.20	±0.02	1.67%

Conclusions of Experimental Section

- In combination with the DAQ, we observe possible explanations to improve the timing resolution
- With the class A detectors, we do not expect to see marked differences in the timing resolution when compared with the class B detector.
- Future Analysis with Class A detectors coming soon
- A desired timing resolution of ~30 nanoseconds therefore depends mostly on a faster data acquisition system.

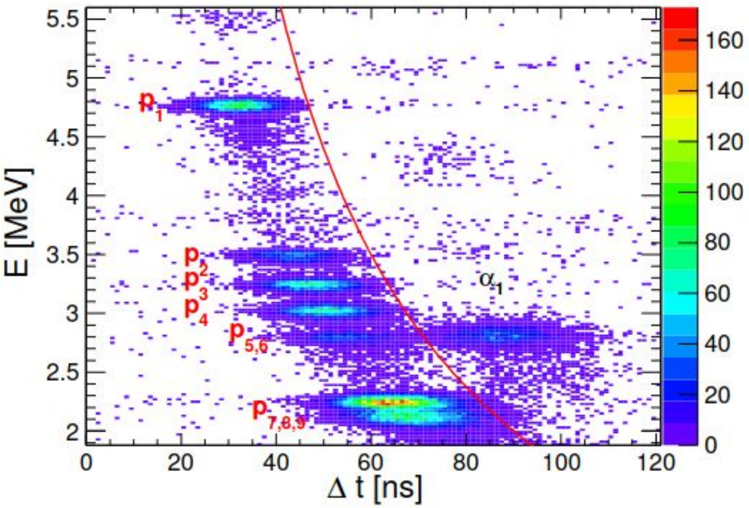

Outlook: GEANT4 simulations of C12+C12 exit channels

Timing ⟶ Distinguish alphas from protons

$$^{12}\mathrm{C} + ^{12}\mathrm{C} \rightarrow ^{20}\mathrm{Ne}^* + \alpha$$

$$^{12}\mathrm{C} + ^{12}\mathrm{C} \rightarrow ^{23}\mathrm{Na}^* + \mathrm{p}$$

$$^{12}\mathrm{C} + \mathrm{d} \rightarrow ^{13}\mathrm{C}^* + \mathrm{p}$$

$$^{12}\mathrm{C} + \mathrm{H} \rightarrow ^{12}\mathrm{C} + \mathrm{H}$$

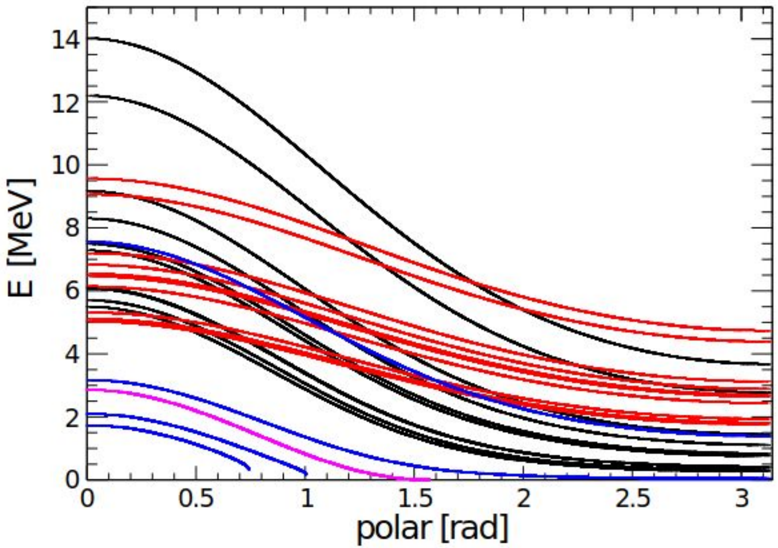

Source: Marcel Heine, Pixel calibration, May 7th 2021

12C+12C→20Ne∗+α,Erel= 2.5 MeV, Isotropic Emission

- r= 5 cm, 7%, centered
- ΔE= 2%
- Micron Super X31.
- 1. bare distribution
- 2. + acceptance effects
- 3. + detector resolution

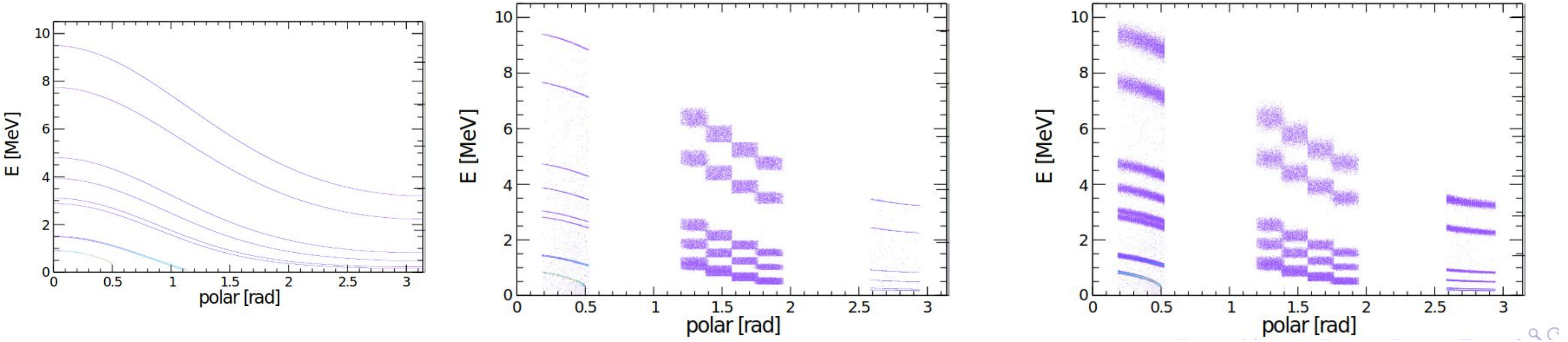

Next step: 12C + 16O

Source: Marcel Heine, Pixel calibration, May 7th 2021

Thank you for your time!

Acknowledgments: A special thanks to Marcel Heine, Sandrine Courtin, Emma Monpribat, and the rest of the DNE and STELLA group.

Bibliography

1. Kenneth Krane, introduction to nuclear physics
2. Illadis, Physics of the stars
3. ”Cauldrons of the Cosmos by Claus E. Rolfs and William S. Rodney[2] Compound Nucleus Reactions
4. https://www.nuclear-power.net/nuclear-power/reactor-physics/nuclear-engineering-fundamentals/neutron-nuclear-reactions/compound-nucleus-reactions/.
5. The STELLA apparatus for particle-Gamma coincidence fusion measurements with nanosecond timing, Heine et al.
6. National Nuclear Data Center https://www.nndc.bnl.gov/nudat2/reCenter.jsp?z=94n=14
7. Survey of heavy-ion fusion hindrance and its implication on astrophysicsC.L. JiangaaPhysics Division, Argonne National Laboratory, Argonne, IL 60439 USA

Appendices

Energy Resolution by position:ohmic

run/peak	Mean	Uncertainty	Sigma	Uncertainty	Relative resolution [%]
1/1	12099.28	.89	59.36	.89	(4.44±0.08)×10-1
1/2	12884.09	1.0	57.20	1.0	(4.44±0.08)×10-1
1/3	13647.32	3.0	59.53	3.1	(4.4±0.2)×10-1
2/1	11846.48	.62	46.72	.65	(3.94±0.05)×10-1
2/2	12624.56	.50	41.00	.48	(3.25±0.04)×10-1
2/3	13358.10	1.6	41.54	1.7	(3.1±0.1)×10-1
3/1	12017.70	2.8	55.62	2.6	(4.6±0.2)×10−1
3/2	12809.46	2.8	52.40	3.0	(4.1±0.2)×10−1
3/3	13538.83	9.6	43.73	11	(3.2±0.8)×10−1

Energy Resolution by position: combined Junction side

run/peak	Mean	Uncertainty	Sigma	Uncertainty	Relative resolution
1/1	18686.8	1.5	92.7	1.4	$(4.96 \pm 0.07) \times 10{-1}$
1/2	19909.3	1.4	88.62	1.4	$(4.45 \pm 0.07) \times 10{-1}$
1/3	21078.1	5.7	96.4	5.2	$(4.6 \pm 0.2) \times 10{-1}$
2/1	18508.8	1.4	95.5	1.4	$(5.16 \pm 0.08) \times 10{-1}$
2/2	19717.4	1.2	89.7	1.2	$(4.55 \pm 0.06) \times 10{-1}$
2/3	20882.8	4.0	95.8	4.6	$(4.6 \pm 0.2) \times 10{-1}$
3/1	18545.7	1.5	98.0	1.4	$(5.29 \pm 0.08) \times 10{-1}$
3/2	19761.7	1.3	94.2	1.3	$(4.77 \pm 0.07) \times 10{-1}$
3/3	20927.4	4.5	94.0	3.8	$(4.5 \pm 0.2) \times 10{-1}$

Energy Resolution by position: combined Junction + Ohmic side

run/peak	Mean	Uncertainty	Sigma	Uncertainty	Relative resolution
1/1	14435.03	.78	67.55	.58	$(4.68\pm0.04)\times10^{-1}$
1/2	15387.80	.80	52.83	.80	$(3.43\pm0.05)\times10^{-1}$
1/3	16299.15	2.5	54.44	2.4	$(3.3\pm0.1)\times10^{-1}$
2/1	14230.04	.79	53.43	.78	$(3.75\pm0.05)\times10^{-1}$
2/2	15160.33	.64	48.72	.62	$(3.21\pm0.04)\times10^{-1}$
2/3	16048.93	2.3	49.50	2.2	$(3.1\pm0.1)\times10^{-1}$
3/1					
3/2					
3/3					

Triple Gauss fit

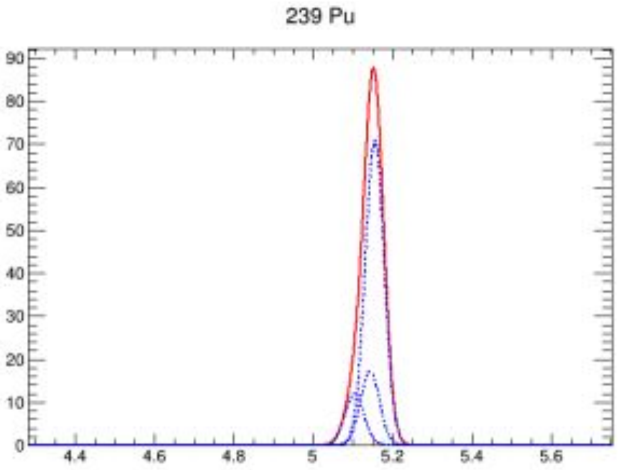

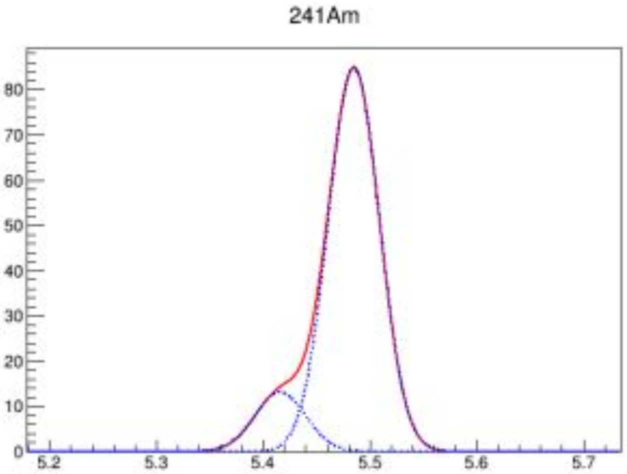

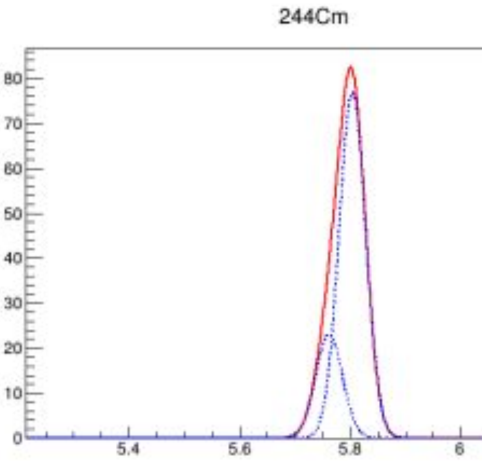

Mesh

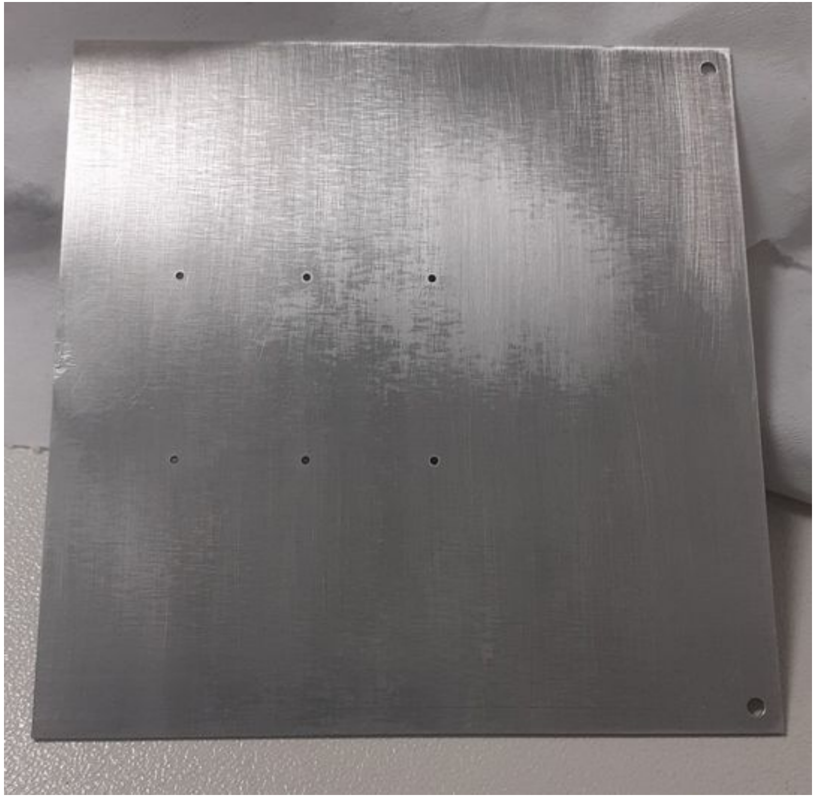

cross sections

S-factors